machines

Article

Assessment of Surface Roughness in Milling of Beech Using a Response Surface Methodology and an Adaptive Network-Based Fuzzy Inference System

Zhaolong Zhu [1,2], Dong Jin [1,2], Zhanwen Wu [3], Wei Xu [1,2,*], Yingyue Yu [2], Xiaolei Guo [3] and Xiaodong (Alice) Wang [4]

1 Co-Innovation Center of Efficient Processing and Utilization of Forest Resources, Nanjing Forestry University, Nanjing 210037, China; njfuzzlong@outlook.com (Z.Z.); kidjin@njfu.edu.cn (D.J.)
2 College of Furnishings and Industrial Design, Nanjing Forestry University, Nanjing 210037, China; njfu_research@outlook.com
3 College of Materials Science and Engineering, Nanjing Forestry University, Nanjing 210037, China; wuzhanwen@njfu.edu.cn (Z.W.); guo.xiao.lei@hotmail.com (X.G.)
4 Department of Wood and Forest Sciences, Laval University, Québec, QC G1V 0A6, Canada; xiaodong.wang@sbf.ulaval.ca
* Correspondence: xuwei@njfu.edu.cn

check for updates

Citation: Zhu, Z.; Jin, D.; Wu, Z.; Xu, W.; Yu, Y.; Guo, X.; Wang, X. Assessment of Surface Roughness in Milling of Beech Using a Response Surface Methodology and an Adaptive Network-Based Fuzzy Inference System. *Machines* **2022**, *10*, 567. https://doi.org/10.3390/machines10070567

Academic Editors: Agathoklis A. Krimpenis, Angelos P. Markopoulos and Dumitru Nedelcu

Received: 16 June 2022
Accepted: 12 July 2022
Published: 14 July 2022

Abstract: This work focused on changes in surface roughness under different cutting conditions for improving the cutting quality of beech wood during milling. A response surface methodology and an adaptive network-based fuzzy inference system were adopted to model and establish the relationship between milling conditions and surface roughness. Moreover, the significant impact of each factor and two-factor interactions on surface roughness were explored by analysis of variance. The specific objective of this work was to find milling parameters for minimum surface roughness, and the optimal milling condition was determined to be a rake angle of 15°, a spindle speed of 3357 r/min and a depth of cut of 0.62 mm. These parameters are suggested to be used in actual machining of beech wood with respect of smoothness surface.

Keywords: wood machining; RSM; milling condition; surface quality; optimization

1. Introduction

Beech wood is widely used for wooden products due to its stable internal structure, high density and good compressive strength performance [1]. Methods always needed to be employed in wood products processing are machining such as turning, sawing [2] and milling [3], and therefore investigations on the cutting performance of material have been favored by researchers around the world [4].

Smoothness of surface is the state of the external layer after machining, and it is also an important evaluation for machining quality [5] At present, surface roughness is mainly used as a crucial evaluation index. The surface roughness of beech wood was studied by Kvietkova et al. [6] during plane milling; their work showed that cutting speed, clearance angle and feeding speed have a significant impact on the surface quality. The effect of tool wear on surface roughness was explored by Kminiak et al. [7] based on beech sawing experiments; they found that tool wear increased as the sawing distance increased, but tool wear has a limited impact on surface smoothness. In the related research of beech milling, an advanced measuring method for surface roughness was developed by Fotin et al. [8]; they showed that milling parameters and anatomical structure have great influence on the surface roughness. Furthermore, changes in surface roughness were investigated by Sütçü and Abdullah [9], and their study indicated that feeding speed and cutting direction are two parameters affecting surface smoothness during beech wood machining. In general, surface roughness is affected predominantly by material properties, cutting speed, tool angle and cutting direction [10,11], and that surface roughness is an important part for final product quality and guaranteed product commercial value [12].

Milling is the most commonly used processing method for wood machining for outstanding machining efficiency [13]. However, due to the lack of research on the milling performance of beech and the non-uniformity of beech wood, there are still quality problems such as abnormal surface damage during industrial beech machining, and how to reduce surface roughness is the key to improve product quality [14,15].

In this work, a series of milling experiments were carried out, and special attention was given to changes in surface roughness under different cutting conditions when the beech wood was milled by straight tooth cutters. This work is expected to provide scientific theoretical guidance for high-quality machining of beech wood.

2. Materials and Methods

As shown in Figure 1, up-milling was performed at a machining center (MGK01, Nanxing Machinery Co., Ltd., Dongguan, China) by diamond cutters with a constant diameter of 140 mm and teeth number of 6 (Table 1, ADC-2717, Leuco precision tooling Co., Ltd., Taicang, China). Beech wood (*Zelkova schneideriana*) was used as the workpiece, and its material properties are listed in Table 2.

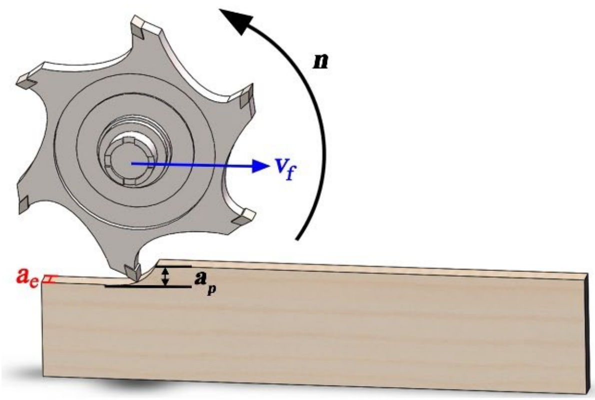

Figure 1. Milling experiment (a_e: cutting width, a_p: depth of cut, V_f: feed speed, n: spindle speed).

Table 1. Geometry and physical parameters of the cutting tools.

No.	Rake Angle	Clearance Angle	Coefficient of Thermal Expansion	Thermal Conductivity	Hardness
1	5°	8°	1.18×10^{-6}	560 W·m^{-1}K^{-1}	8000 HV
2	10°	8°			
3	15°	8°			

Table 2. Material properties of beech wood.

Density	Modulus of Elasticity	Moisture Content	Bending Strength
0.7 g/cm^3	9681.3 MPa	11.2%	92.5 MPa

In this work, surface roughness *Ra* was in focus, changes in surface roughness under different cutting conditions were explored by a response surface methodology (RSM) using Design-Expert software (Version 12, Stat-Ease Inc., Minneapolis, MN, USA) and an adaptive network-based fuzzy inference system using (Version R2018A, MathWorks Inc., Natick, MA, USA). Surface roughness was acquired by a surface roughness meter (S-NEX001SD-12, Tokyo Seimitsu Co., Ltd., Tokyo, Japan) under different cutting conditions. The profile of the machined surface was detected by a diamond probe with a radius of 2 µm, and the measuring direction was parallel to feeding direction with a speed of 1 mm/s, and the measuring distance was 10 mm. Surface roughness *Ra* was processed by ACCTee software (Accretech, Tokyo Seimitsu Co., Ltd., Tokyo, Japan) with Gaussian filtering. The experimental design was given in Table 3—each combination of cutting condition was repeated five times, and the average value of *Ra* was obtained based on the five samples.

Table 3. Experimental design and results.

No.	Rake Angle (°)	Spindle Speed (r/min)	Depth of Cut (mm)	*Ra* (Actual) (μm)	*Ra* (RSM) (μm)	Pred. Error (RSM)	*Ra* (ANFIS) (μm)	Pred. Error (ANFIS)
1	5	2500	0.5	4.058	4.293	5.47%	4.047	−0.28%
2	5	5000	0.5	3.797	3.552	−6.98%	3.802	0.14%
3	5	7500	0.5	3.206	3.084	−3.96%	3.225	0.58%
4	5	2500	1.0	4.604	4.813	4.34%	4.611	0.15%
5	5	5000	1.0	4.341	3.954	−9.79%	4.339	−0.05%
6	5	7500	1.0	3.377	3.367	−0.30%	3.394	0.51%
7	5	2500	1.5	4.927	5.391	8.61%	4.924	−0.05%
8	5	5000	1.5	4.368	4.414	1.04%	4.357	−0.26%
9	5	7500	1.5	4.456	3.709	−0.14%	4.429	−0.61%
10	10	2500	0.5	3.711	3.747	0.96%	3.706	−0.16%
11	10	5000	0.5	3.231	3.468	6.83%	3.880	20.09%
12	10	7500	0.5	3.206	3.461	7.37%	3.241	1.08%
13	10	2500	1.0	3.854	4.162	7.40%	3.854	0.01%
14	10	5000	1.0	3.765	3.765	0.00%	3.779	0.36%
15	10	7500	1.0	3.447	3.639	5.28%	3.809	10.51%
16	10	2500	1.5	4.891	4.636	−5.50%	4.887	−0.08%
17	10	5000	1.5	3.951	4.121	4.13%	4.593	16.25%
18	10	7500	1.5	3.913	3.877	−0.93%	3.921	0.21%
19	15	2500	0.5	2.793	2.066	−35.19%	2.402	−14.00%
20	15	5000	0.5	2.294	2.248	−2.05%	2.288	−0.28%
21	15	7500	0.5	2.28	2.702	15.62%	3.218	41.12%
22	15	2500	1.0	2.366	2.376	0.42%	2.368	0.08%
23	15	5000	1.0	3.652	2.440	−49.67%	3.037	−16.83%
24	15	7500	1.0	2.984	2.776	−7.49%	2.986	0.08%
25	15	2500	1.5	4.033	2.745	−46.92%	2.831	−29.82%
26	15	5000	1.5	2.446	2.691	9.10%	2.453	0.30%
27	15	7500	1.5	2.984	2.908	−2.61%	3.524	18.09%

3. Results and Discussion

3.1. A RSM for Surface Roughness

A response surface model was established based on the obtained beech milling surface roughness data. For mathematical modeling, two-factor interaction (2FI) and quadratic models are commonly used [16]. The fitting degrees of these three types of models are given in Table 4. Linear and quadratic models were suggested, but the R^2 and adjusted R^2 of the quadratic model were 0.96 and 0.91, respectively, and its goodness of fit was higher than that of the linear model. Therefore, the quadratic term form was chosen to establish the response surface model, similar to in a previous work [17].

Table 4. Model fit statistics table.

Source	Std. Dev.	R^2	Adjusted R^2	
Linear	0.46	0.69	0.62	Suggested
2FI	0.42	0.80	0.68	/
Quadratic	0.22	0.96	0.91	Suggested

Fitted statistics of the machined surface roughness are shown in Table 5. The model's coefficient of determination R^2 and adjusted R^2 are 0.96 and 0.91, respectively, and they are very close to 1. Std. Dev. is the experimental standard deviation, it can reflect the degree of dispersion of a dataset. Coefficient of variation (C.V.%) is the ratio of the standard deviation of the original data to the mean of the original data, which was very low. Comparison of the predicted values and actual values in Figure 2 did not show a significant variant point and this shows that the model was fitted, and can be used to establish a mathematical model of surface roughness.

Table 5. Model fit statistics of *Ra*.

Model	Std. Dev.	Mean	C.V.%	R^2	Adjusted-R^2	Adeq Precision
Ra	0.2216	3.58	6.2	0.9604	0.9095	15.0924

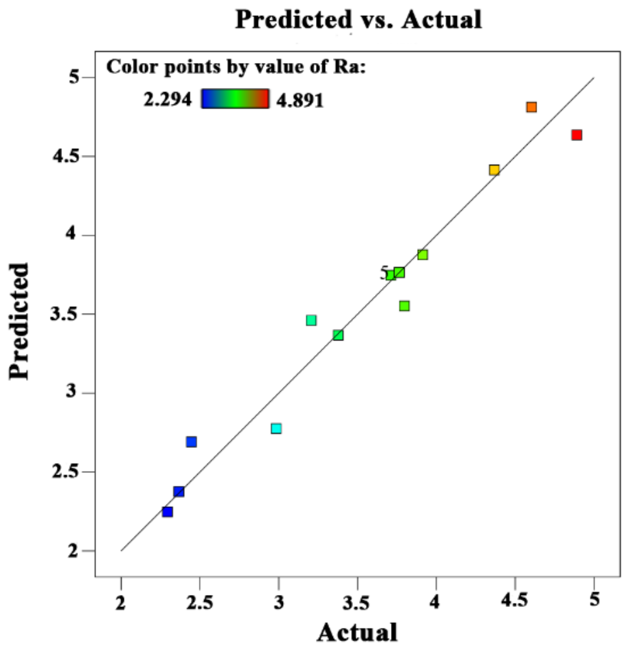

Figure 2. Predicted and actual value of *Ra*.

The machined surface roughness of beech was obtained as shown in Equation (1).

$$\begin{aligned} Ra = 3.77 - 0.757\alpha - 0.2645n + 0.3263a_p + 0.4613\alpha n - 0.1048\alpha a_p \\ -0.1183na_p - 0.5681\alpha^2 + 0.1359n^2 + 0.0294{a_p}^2 \end{aligned} \quad (1)$$

where α is rake angle in °, n is the spindle speed in r/min, a_p is depth of cut in mm.

The ANOVA results of the model are shown in Table 6. The F-value was 18.88, and a p-value < 0.05 indicated that this model was significant. The cutting parameters represented by A, B, and C in the table are tool rake angle (α), spindle speed (n) and depth of cut (a_p).

Table 6. Result of ANOVA for surface roughness *Ra*.

Source	Sum of Squares	df	Mean Square	F-Value	*p*-Value	
Model	8.34	9	0.9267	18.88	0.0004	Significant
A-α	4.58	1	4.58	93.38	<0.0001	Significant
B-n	0.5471	1	0.5471	11.14	0.0125	Significant
C-a_p	0.8515	1	0.8515	17.34	0.0042	Significant
AB	0.851	1	0.851	17.33	0.0042	Significant
AC	0.0439	1	0.0439	0.894	0.3759	Insignificant
BC	0.0559	1	0.0559	1.14	0.3212	Insignificant
A^2	1.36	1	1.36	27.68	0.0012	Significant
B^2	0.0777	1	0.0777	1.58	0.2486	Insignificant
C^2	0.0036	1	0.0036	0.074	0.7934	Insignificant
Pure Error	0	4	0			
Total	8.68	16				

It can be seen from Figure 3 that *Ra* is positively correlated with the depth of cut, and negatively correlated with spindle speed and tool rake angle, whereas the influence of the cutting parameter on *Ra* was ranked as $\alpha > a_p > n$. In the RSM model, ANOVA can be used to explore the impact of variation from different sources to the total variation, namely, the impacting degree of a factor or two-factor interactions on surface roughness. Meanwhile, the curve distribution density of a 2D surface plot can indicate the significant impact of two-factor interactions on surface roughness. Thus, combined with Table 6 and Figure 4, the cutting parameters (α, n, and a_p) have a significant impact on *Ra* ($p < 0.05$), and the influence of the quadratic interaction term $\alpha \times n$ on *Ra* is significant ($p < 0.05$). In the analysis of the impacting degree of the quadratic interaction term on *Ra*, Figure 4a shows the influence of $\alpha \times n$ on *Ra*; it can be found that rake angle has a higher impacting degree than spindle speed on *Ra*; Figure 4b shows the influence of $\alpha \times a_p$ on *Ra*, rake angle has a higher impacting degree than depth of cut on *Ra*; Figure 4c displays the influence of $n \times a_p$ on *Ra*, it can be found that depth of cut has a higher impacting degree than spindle speed on *Ra*.

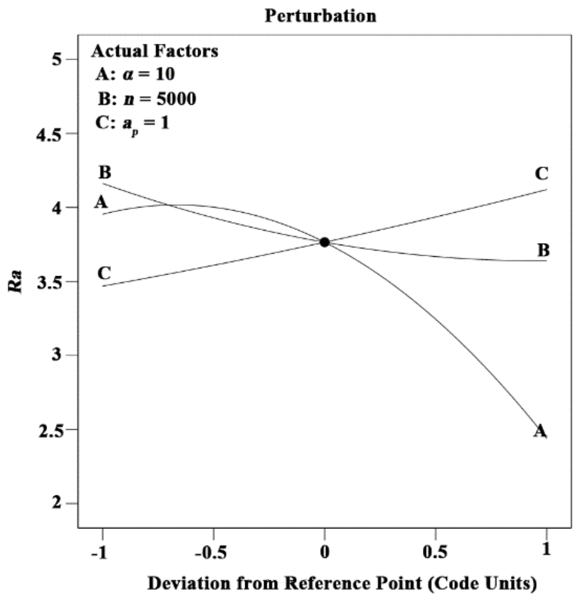

Figure 3. Effect of cutting parameters on *Ra*.

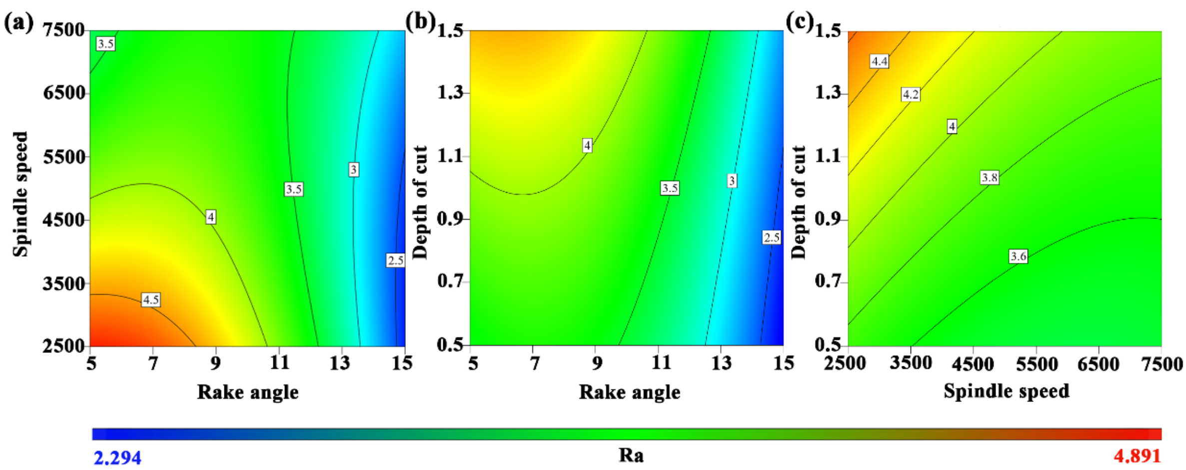

Figure 4. The 2D surface plot displaying the effect of cutting parameters on *Ra*: (**a**) spindle speed and rake angle; (**b**) depth of cut and rake angle; (**c**) depth of cut and spindle speed.

Combined with the ANOVA results and Figure 5, the quadratic term α^2 of the cutting parameters has a significant effect on *Ra* ($p < 0.05$), then the order of influence of the quadratic term is as follows: $\alpha^2 > n^2 > {a_p}^2$.

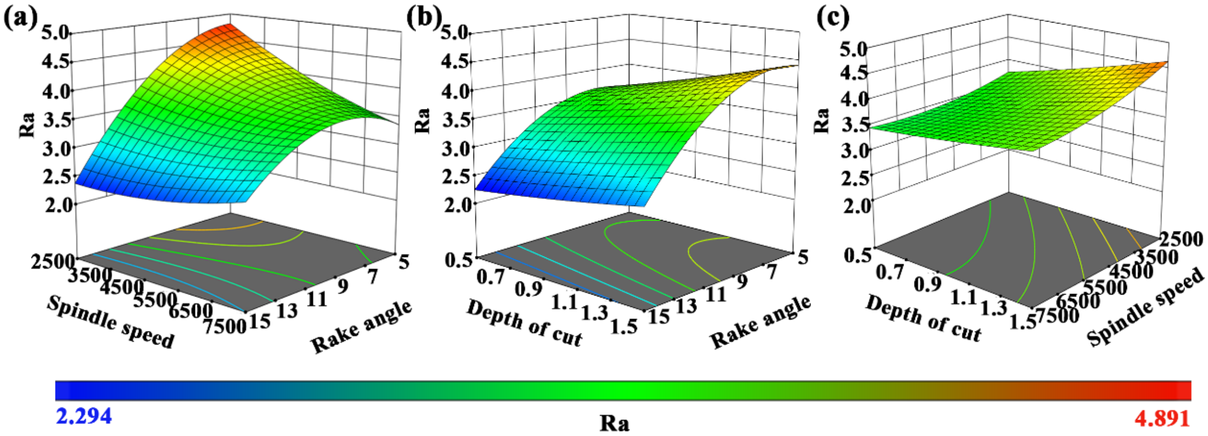

Figure 5. The 3D surface plot showing the effect of cutting parameters on *Ra*: (**a**) spindle speed and rake angle; (**b**) depth of cut and rake angle; (**c**) depth of cut and spindle speed.

3.2. ANFIS Methodology for Surface Roughness

The Adaptive Network-based Fuzzy Inference System (ANFIS) was proposed by Jang [18] in 1993, where they used fuzzy if-then rules to map the complex non-linear relationship between input and output variables, and used a set of input and output data to train the neural network [19,20]. This technology's ability is to compute complex problems with large uncertainties. It is a multi-layer structure based on hybrid learning that utilizes Least Squares Estimation (LSE) and Gradient Descent (GD) methods to construct input–output mappings. The standard two-pass learning process of ANFIS consists of a forward pass in which the outputs of nodes are computed until the fourth layer, where the LSE updates the backward parameters. While in the backward pass, the error propagates forward until the first layer, where GD tunes the premise parameters, which are membership function parameters. The ANFIS architecture consists of five distinct layers. Figure 6 shows the functional details of each layer of ANFIS. Function of Layer 1: Fuzzy the input features x and y with the membership function to obtain a membership grade in the [0, 1] interval; the output calculation of each node is shown in Equation (2) [21], which is an example of a generalized bell-shaped membership function. The premise parameter set (j_i, k_i, l_i) defines the shape of the membership function.

$$M_i^1 = \mu Ai(x) = \frac{1}{1 + \left[\left|\frac{x - l_i}{j_i}\right|^{2k_i}\right]} \tag{2}$$

where (j_i, k_i, l_i) is the parameter set. The change in these parameters is A_{i} in various forms, x is the input feature, and $\mu Ai(x)$ is a ball-shaped function and it has a maximum value of 1 and a minimum value of 0.

Function of Layer 2: Multiply the membership of each feature to obtain the firing strength of each rule, as shown in Equation (3) [22]

$$M_i^2 = wi = \mu Ai(x) \times \mu Ai(y) \tag{3}$$

Function of Layer 3: Normalize the trigger strength of each rule obtained by the previous layer to represent the trigger proportion of the rule in the entire rule base, that is, the probability of using this rule in the entire reasoning process. It can be calculated by Equation (4) [21,22].

$$M_i^3 = \overline{wi} = \frac{wi}{w1 + w2}, i = 1,\ 2 \tag{4}$$

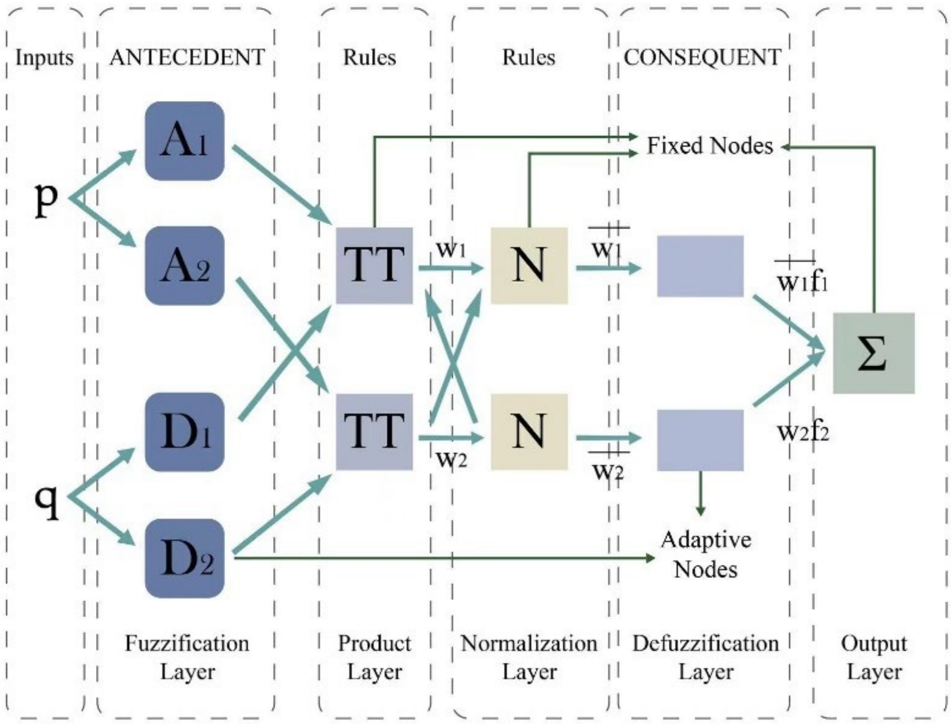

Figure 6. Adaptive fuzzy neural network structure.

Function of Layer 4: Called the deburring layer, it is composed of adaptive nodes, and its function is shown in Equation (5).

$$M_i^4 = \overline{wi} f_i = \overline{wi}(p_i x + q_i y + r_i) \tag{5}$$

where p_i, q_i, and r_i are consequent parameters, and $\overline{wi}$ is the output of Layer 3.

Function of Layer 5: Obtain the exact output; the final system output is the weighted average of the results of each rule by Equation (6) [22,23].

$$M_i^5 = finalO/P = \sum_i \overline{wi} f_i = \frac{\sum_i \overline{wi} f_i}{\sum_i \overline{wi}} \tag{6}$$

The ANFIS architecture for surface roughness is shown in Figure 7. The input variables are rake angle, spindle speed and depth of cut, and the output variable is the machined surface roughness. From the 27 combinations, 19 combinations were selected as training data (approximately 70%), and the remaining 8 combinations (approximately 30%) were used as test data.

Figure 8 shows the training and test graphs generated from the training input set and the test dataset. For the established ANFIS model, 100 learning intervals (epochs) were performed on 19 training datasets. The trained ANFIS network was loaded and all the data were predicted to obtain the error data predicted by the model, which is shown in Table 6. The overall error of the model is small, and there are only a few groups of large deviations, which are within an acceptable range, so it is feasible to use ANFIS to predict *Ra*.

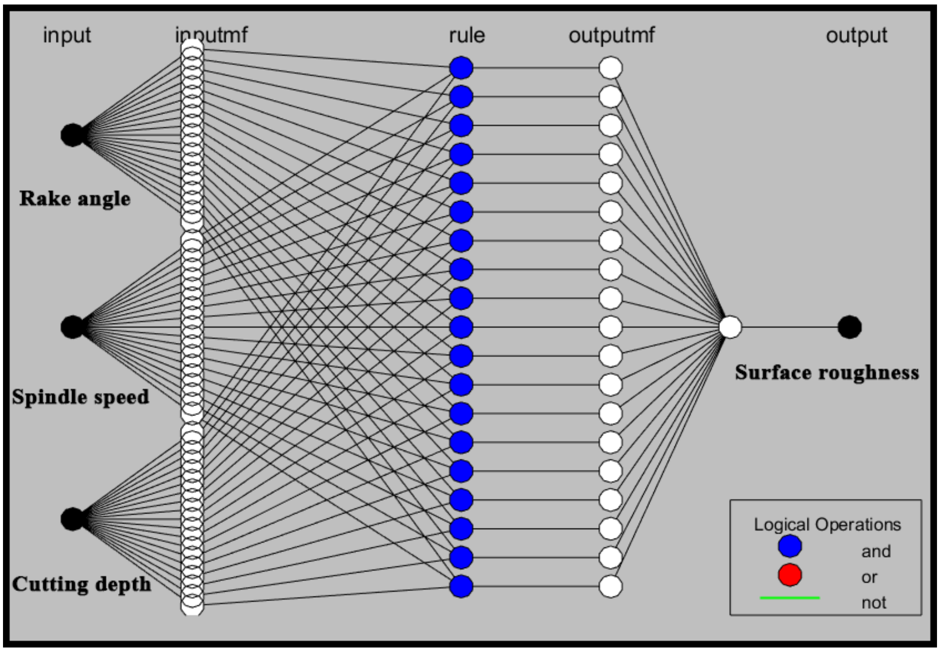

Figure 7. ANFIS architecture for surface roughness.

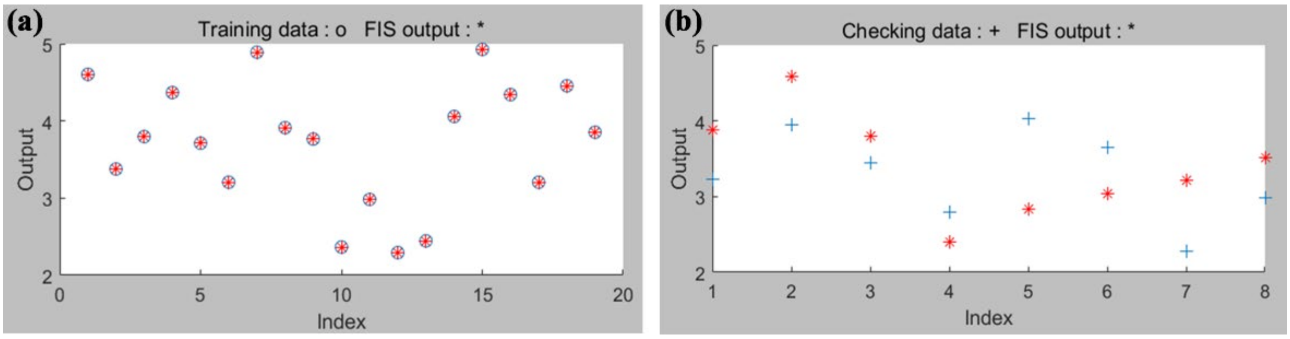

Figure 8. Plot of (**a**) training data and (**b**) test data.

Figure 10 shows the influence of cutting parameters on *Ra* obtained by the ANFIS model; this is consistent with the law obtained by the RSM model (Figure 3), of which *Ra* is positively correlated with depth of cut, and negatively correlated with spindle speed and tool rake angle.

The *Ra* of the predicted ANFIS values and real-time experimental values were facilitated by the Sugeno rule viewer, which effectively supports tracking of predetermined input–output datasets and supervised learning processes. 19 rules between input and output values are defined in Figure 9.

In the analysis of the influence degree of the secondary interaction term on *Ra* obtained by the ANFIS model and the interactive effects of spindle speed and tool rake angle on Ra, tool rake angle is the main influence. Among the interactive effects of depth of cut and tool rake angle on *Ra*, tool rake angle is the main influence; and among the interactive effects of depth of cut and spindle speed on Ra, depth of cut is the main influence. Obviously, this is highly consistent with the trend obtained by the RSM model (Figures 5 and 11).

3.3. Optimization and Verification for High-Quality Machining

After processing, the surface roughness of beech wood is an important measure to evaluate its machined quality, which is related to subsequent use and surface decoration processes [24,25]. In the above analysis, cutting parameters and surface quality were closely related. Appropriate machining parameters were predicted using response surface and adaptive fuzzy neural networks, and the goal was to obtain the best machining surface quality.

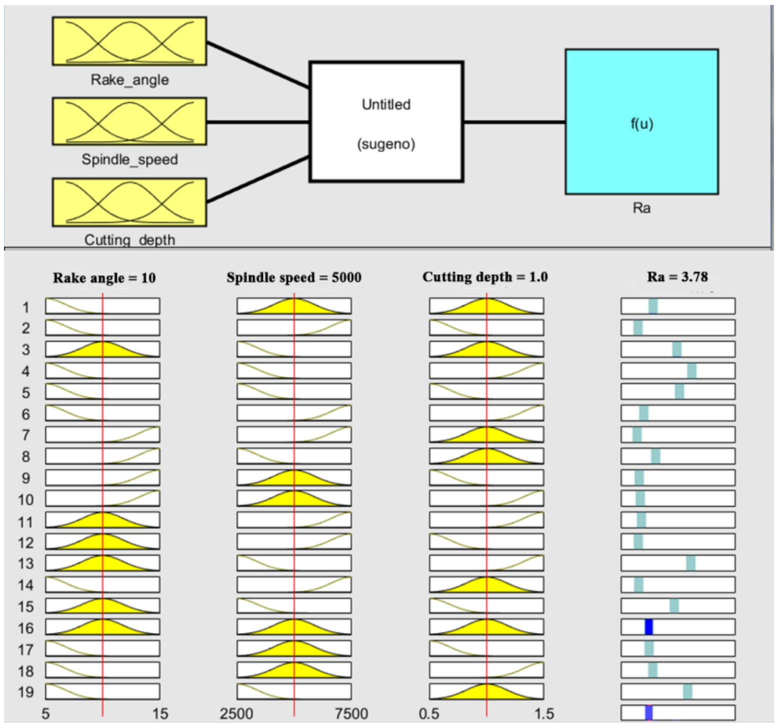

Figure 9. Sugeno inference for *Ra*.

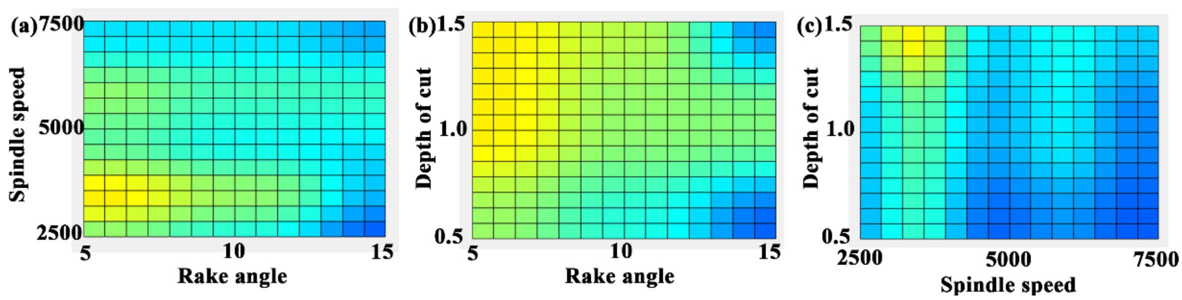

Figure 10. The 2D surface plot from ANFIS about the effect of cutting parameters on *Ra*: (**a**) spindle speed and rake angle, (**b**) depth of cut and rake angle, and (**c**) depth of cut and spindle speed.

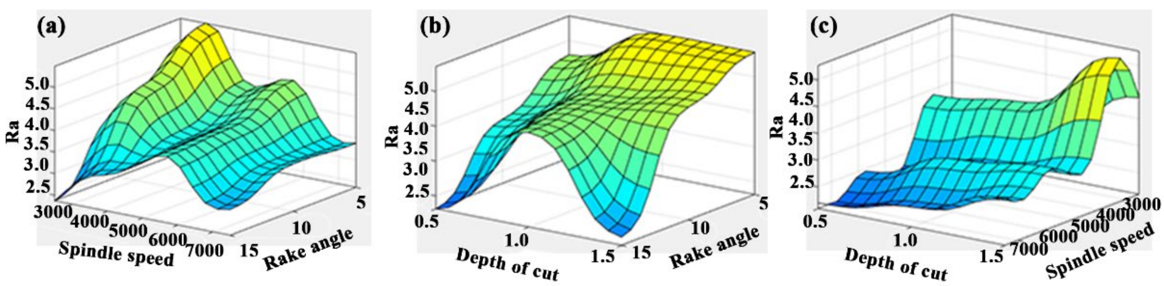

Figure 11. The 3D surface plot from ANFIS about the effect of cutting parameters on *Ra*: (**a**) spindle speed and rake angle, (**b**) depth of cut and rake angle, and (**c**) depth of cut and spindle speed.

The input variables in predicting optimal parameters are rake angle, depth of cut and spindle speed, respectively. Meanwhile, the optimal parameter ranges are as follows: a rake angle of 5–15°, a spindle speed of 2500–7500 r/min, and a depth of cut of 0.5–1.5 mm.

Based on the experimental results, it can be found that the red points in Figure 12 are the most suitable locations for each parameter prediction, and the prediction points are also shown in Figure 13. In order to verify the reliability of the predicted results, the error of the model prediction obtained by verification experiment is shown in Table 7, the error value is −5.24% within acceptable limits. Moreover, it was observed that surface roughness at the optimal processing parameters was smaller than the minimum value obtained in the original experimental design, it further indicated that the model prediction result was reliable. Therefore, the optimal processing parameters for beech wood processing were a rake angle of 15°, a spindle speed of 3357 r/min, a depth of cut of 0.62 mm, and an optimal surface roughness of 2.383 μm.

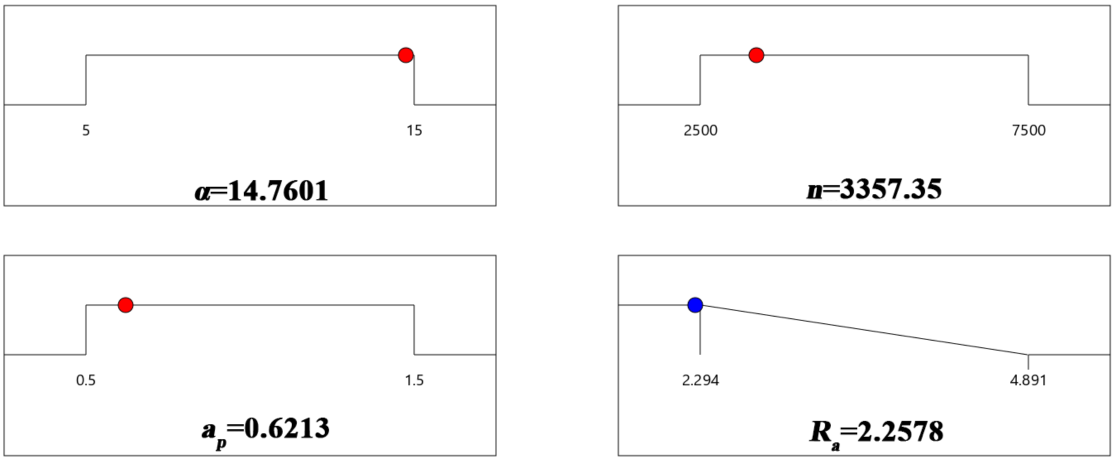

Figure 12. Prediction of cutting parameters.

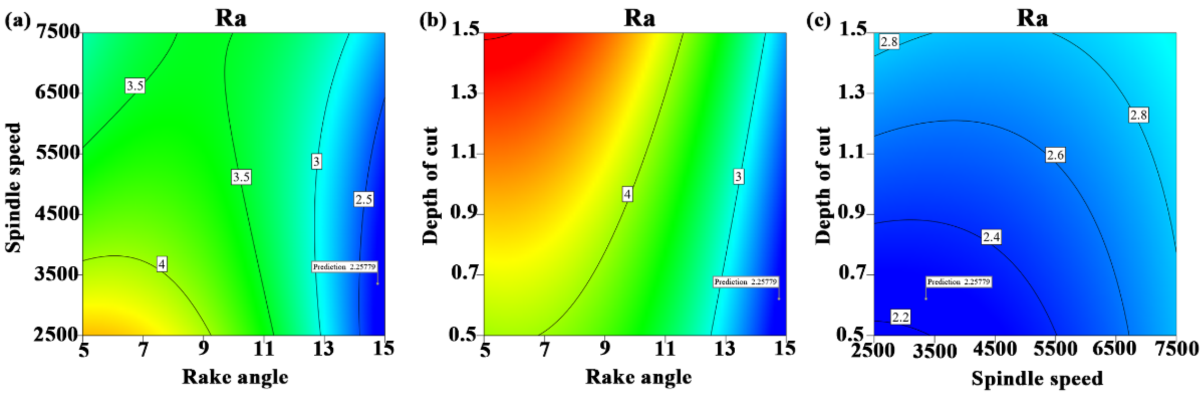

Figure 13. Response surface prediction point location map. (**a**) spindle speed and rake angle, (**b**) depth of cut and rake angle, and (**c**) depth of cut and spindle speed.

Table 7. Model prediction error rate.

Tests	Rake Angle (°)	Spindle Speed (r/min)	Depth of Cut (mm)	Surface Roughness (μm)
Prediction	15	3357	0.62	2.258
Verification	15	3357	0.62	2.383
Error rate	\	\	\	−5.24%

4. Conclusions

In this paper, a beech wood milling test was used to make prediction models. The cutting parameters were rake angle, spindle speed and depth of cut, and special focus was given to surface roughness *Ra* at difference cutting conditions. Based on the experiment results, a RSM model was established, and the influence degree of each input parameter primary term, interaction term and quadratic term on *Ra* is systematically analyzed. At the same time, the adaptive neuro-fuzzy inference system (ANFIS) was used to predict and analyze the cutting data, and the obtained results were compared with the RSM. The following conclusions were obtained:

(1) *Ra* is positively correlated with depth of cut, and negatively correlated with spindle speed and tool rake angle; meanwhile, the degree of influence of the cutting parameter on *Ra* was ranked as $\alpha > a_p > n$; the degree of influence of the interaction term on *Ra* was ranked as $\alpha \times n > n \times a_p > \alpha \times a_p$; the order of influence of the quadratic term of the cutting parameters was $\alpha^2 > n^2 > {a_p}^2$.
(2) The established ANFIS model is reliable for *Ra* prediction. Based on the Sugeno inference system, the non-linear modeling prediction becomes simple and reliable.
(3) The relationship between the influence of each cutting parameter on *Ra* obtained by RSM and ANFIS is highly consistent, which not only proves the reliability of the model, but also the reliability of the obtained influence law.
(4) With the optimal cutting quality as the goal, the optimal milling condition is a tool with a rake angle of 15°, a spindle speed of 3357 r/min and a depth of cut of 0.62 mm.

Surface roughness, cutting energy, tool wear, chip formation, etc., are important indicators to evaluate the cutting performance of beech, and this needs further research in the follow-up.

Author Contributions: Conceptualization, D.J. and Z.W.; methodology, Z.W.; software, Y.Y.; validation, X.W., Y.Y. and Z.Z.; formal analysis, W.X.; investigation, Y.Y.; resources, X.G.; data curation, Z.Z.; writing—original draft preparation, W.X.; writing—review and editing, Y.Y.; visualization, X.G.; supervision, W.X.; project administration, Z.Z.; funding acquisition, W.X. All authors have read and agreed to the published version of the manuscript.

Funding: This research was supported by the National Natural Science Foundation of China [grant number 31971594]; the Natural Science Foundation of the Jiangsu Higher Education Institutions of China [21KJB220009]; the Self-Made Experimental and Teaching Instruments of Nanjing Forestry University in 2021 [nlzzyq202101]; the project from Technology Innovation Alliance of Wood/Bamboo Industry [TIAWBI2021-08]; the International Cooperation Joint Laboratory for Production, Education, Research and Application of Ecological Health Care on Home Furnishing.

Institutional Review Board Statement: Not applicable.

Informed Consent Statement: Not applicable.

Data Availability Statement: Not applicable.

Conflicts of Interest: The authors declare no conflict of interest.

References

1. Zeng, K.; Gauthier, D.; Lu, J.; Flamant, G. Parametric study and process optimization for solar pyrolysis of beech wood. *Energy Convers. Manag.* **2015**, *106*, 987–998. [CrossRef]
2. Xiong, X.; Yue, X. Research and application progress of home intelligent manufacturing technologies in China. *J. For. Eng.* **2022**, *7*, 26–34.
3. Zhang, F.; Wu, Z.; Ding, J.; Guo, X.; Cao, P.; Zhu, Z. Milling performance of stone-plastic composite with diamond cutters. *Mater. Werkst.* **2021**, *52*, 1307–1318. [CrossRef]
4. Ren, J.; Xiong, X.; Zhao, J.; Fei, J.; Zhang, J. Research on standardized design of solid wood customized cabinet doors. *J. For. Eng.* **2022**, *7*, 197–204.
5. Yang, X.; Xiong, X. Information collection and application of furniture production line using radio frequency identification technology. *J. For. Eng.* **2022**, *7*, 180–186.
6. Kvietkova, M.; Gasparik, M.; Gaff, M. Effect of thermal treatment on surface quality of beech wood after plane milling. *Bioresources* **2015**, *10*, 4226–4238. [CrossRef]
7. Kminiak, R.; Gasparik, M.; Kvietkova, M. The dependence of surface quality on tool wear of circular saw blades during transversal sawing of beech wood. *Bioresources* **2015**, *10*, 7123–7135. [CrossRef]
8. Fotin, A.; Cismaru, I.; Cismaru, M.; Cosereanu, C.; Curtu, I. The influence of the profiled milling parameters to the quality of the surface. *Ann. DAAAM Proc.* **2010**, *20*, 413–414.

9. Sütçü, A. Investigation of parameters affecting surface roughness in cnc routing operation on wooden EGP. *Bioresources* **2013**, *8*, 795–805. [CrossRef]
10. Hu, W.; Liu, Y.; Li, S. Characterizing mode I fracture behaviors of wood using compact tension in selected system crack propagation. *Forests* **2021**, *12*, 1369. [CrossRef]
11. Fang, L.; Zeng, J.; Zhang, X.; Wang, D. Effect of veneer initial moisture content on the performance of polyethylene film reinforced decorative veneer. *Forests* **2021**, *12*, 102. [CrossRef]
12. Zhong, Z.W.; Hiziroglu, S.; Chan, C. Measurement of the surface roughness of wood based materials used in furniture manufacture. *Measurement* **2013**, *46*, 1482–1487. [CrossRef]
13. Fang, L.; Zhang, X.; Zhang, Y.; Tang, Q. Manufacturing and interfacial bonding behavior of EVA film reinforced flexible decorative veneer. *Wood Fiber Sci.* **2021**, *53*, 194–205. [CrossRef]
14. Li, R.; Yang, F.; Wang, X. Modeling and Predicting the Machined Surface Roughness and Milling Power in Scot's Pine Helical Milling Process. *Machines* **2022**, *10*, 331. [CrossRef]
15. Jin, D.; Wei, K. Machinability of Scots Pine during Peripheral Milling with Helical Cutters. *Bioresources* **2022**, *16*, 8172–8183. [CrossRef]
16. Li, R.; He, C.; Xu, W.; Wang, X. Prediction of surface roughness of CO_2 laser modified poplar wood via response surface methodology. *Maderas-Cienc. Tecnol.* **2022**, *24*.
17. Li, R.; He, C.; Xu, W.; Wang, X. Modeling and optimizing the specific cutting energy of medium density fiberboard during the helical up-milling process. *Wood Mater. Sci. Eng.* **2022**, 1–8. [CrossRef]
18. Jang, J.S. ANFIS: Adaptive-network-based fuzzy inference system. *IEEE Trans. Syst. Man Cybern.* **1993**, *23*, 665–685. [CrossRef]
19. Ren, J.; Xiong, X.; Tang, Y.; Zhao, J.; Fei, J.; Zhang, J. Furniture part family division of customized wooded cabinet doors using multi-attribute cross clustering. *J. For. Eng.* **2022**, *7*, 187–193.
20. Shekarian, E.; Gholizadeh, A.A. Application of adaptive network based fuzzy inference system method in economic welfare. *Knowl. Based Syst.* **2013**, *39*, 151–158. [CrossRef]
21. Karaboga, D.; Kaya, E. Adaptive network based fuzzy inference system (ANFIS) training approaches: A comprehensive survey. *Artif. Intell. Rev.* **2019**, *52*, 2263–2293. [CrossRef]
22. Yang, H.; Hasanipanah, M.; Tahir, M.M.; Bui, D.T. Intelligent prediction of blasting-induced ground vibration using AN FIS optimized by GA and PSO. *Nat. Resour. Res.* **2020**, *29*, 739–750. [CrossRef]
23. Zhou, J.; Li, C.; Arslan, C.A.; Hasanipanah, M.; Amnieh, H.B. Performance evaluation of hybrid FFA-ANFIS and GA-ANFIS models to predict particle size distribution of a muck-pile after blasting. *Eng. Comput.* **2021**, *37*, 265–274. [CrossRef]
24. Mo, X.; Zhang, X.; Fang, L.; Zhang, Y. Research progress of wood-based panels made of thermoplastics as wood adhesives. *Polymers* **2021**, *14*, 98. [CrossRef] [PubMed]
25. Nalbant, M.; Gokkaya, H.; Sur, G. Application of taguchi method in the optimization of cutting parameters for surface roughness in turning. *Mater. Design* **2007**, *28*, 1379–1385. [CrossRef]